Paper No. 731. (quote when citing this article)
Eleventh World Conference on Earthquake Engineering
ISBN: 0 08 042822 3

DEPTH-DEPENDENT SPATIAL VARIATION OF GROUND MOTION BASED ON SEISMIC ARRAY RECORDS

Hirokazu NAKAMURA

Graduate Student, Institute of Industrial Science, The University of Tokyo,
7-22-1 Roppongi, Minato-ku, Tokyo, 106 Japan

ABSTRACT

The spatially varying earthquake ground motion has a spatial variation usually increasing due to wave propagation inside the ground. It is important for the design of spatially-extended underground structures to get information on the spatial variation in near-surface soil layers. The aim of this study is to examine the depth-dependence of the spatial variation described by the coherence function, based on twelve earthquake events observed at ground levels –1 m, –10 m, and –20 m in the Chiba array. To quantify the spatial variation at each depth in great detail, some spatial variation parameters are analyzed by using the coherence function model proposed in this study. Then the spatial variation parameters, that is, the spatial correlation coefficient and the normalized fluctuation scale, are modeled as a function of depth. The results show that the spatial correlation increases with the decrease of depth level beneath the surface. Also, it is indicated that, within the limitations of the area considered, the amount of the spatial variation at the surface for horizontal and up-down components would be about 18 per cent and 12 per cent respectively, and that the spatial variation from the surface down to the –20 m level is more than 20 per cent with respect to that in the deeper soil layers.

KEYWORDS

earthquake ground motion; Chiba array; spatial variation (correlation); underground motion; coherence function.

INTRODUCTION

Grasping the spatial variation characteristics of earthquake ground motion is important for the prediction of the behavior of underground facilities during an earthquake. The earthquake ground motion varies in space. Two time histories of an array observation record will never coincide so long as the observation points differ (Katayama, 1991). It is usually the coherence function that describes the similarity of two time histories in the frequency domain. Thus, the coherence function is utilized to characterize the spatial variation. Array observation records provide useful information for evaluating the spatial variation of earthquake ground motion. The spatial variation at the ground surface has been extensively studied by using a coherence function based on array records by Harada (1984), Harichandran and Vanmarcke (1986), Loh and Yeh (1988), Sawada and Kameda (1988), Hao (1989), Kataoka *et al.* (1990), Abrahamson *et al.* (1991), Lu *et al.* (1994) and Nakamura and Yamazaki (1995). The spatial variation due to an inhomogeneous medium was numerically investigated by the finite difference or element analysis assigning the perturbation to the seismic velocity structure by Menke *et al.* (1991) and Sato and Kawase (1992). These studies were only qualitative, and the results should be verified using array observation records. Compared with the number of studies devoted to the spatial variation at the ground surface, those of the spatial variation of the underground motion are very few in number, owing to the limitations of availability of related array data.

To quantify the spatial variation of underground motion, this paper is aimed at the examination of the depth-dependence of the spatial variation for free-field earthquake ground motion in terms of the spatial variation parameters, based on twelve earthquake events observed at the Chiba array, Japan. The spatial variation parameters are analyzed using the

array records at the ground levels, –1 m, –10 m, and –20 m. These spatial variation parameters are the coherence function, spatial correlation coefficient and the normalized fluctuation scale. They are modeled for a better understanding of the depth-dependent spatial variation of earthquake ground motion.

ESTIMATION OF SPATIAL VARIATION PARAMETERS

Ground motion records at the depth level, z, are vectorially converted into the radial and transverse directions. The spatial variation of the ground motion for each of the three vibration components, i.e., radial (j = R), transverse (j = T), and up-down (j = U), is taken into account. In this study, assuming the strong motion parts of the acceleration records to be statistically homogeneous and stationary over the area and time duration considered, the one-sided power spectra G_{jj} are computed by use of that limited part. Then the variance of the ground motion is

$$\sigma_{jj}^2(z) = \int_f G_{jj}(0, 0, z, f)\, df, \tag{1}$$

and then the unit-area power spectrum is

$$g_{jj}(0, 0, z, f) = G_{jj}(0, 0, z, f)/\sigma_{jj}^2(z). \tag{2}$$

Since only a limited portion of time history is analyzed, the coherence function is obtained from the smoothed power spectra at specified locations, $\boldsymbol{x}$ and $\boldsymbol{x} + \boldsymbol{\xi}$. Using the cross power spectrum, the coherence function is defined as

$$\gamma_{jj}(\xi_r, \xi_t, z, f) = \left|G_{jj}(\xi_r, \xi_t, z, f)\right| / G_{jj}(0, 0, z, f), \tag{3}$$

at the separation vector, (ξ_r, ξ_t), and the frequency, f, converted from the time lag. The coherence function becomes unity for all frequency if the separation vector is zero:

$$\gamma_{jj}(0, 0, z, f) = 1.0. \tag{4}$$

The coherence function gives us all information about the horizontal spatial variation of earthquake ground motion. Using simple estimates, that provide us with the more condensed information is sometimes convenient. We call the simple estimates spatial variation parameters (Vanmarcke, 1983; Harada, 1984). As one of the spatial variation parameters, the correlation area is defined by the integral of coherence function over separation vectors:

$$\theta_{jj}(z, f) = \iint_{\xi} \gamma_{jj}(\xi_r, \xi_t, z, f)\, d\xi_r d\xi_t. \tag{5}$$

Also the spatial correlation coefficient is expressed as

$$\eta_{jj}(\xi_r, \xi_t, z) = \int_f g_{jj}(0, 0, z, f)\ \gamma_{jj}(\xi_r, \xi_t, z, f)\ df, \tag{6}$$

that shows a weighted integration of the coherence function by the unit-area power spectrum. Furthermore by integrating the spatial correlation coefficient, the fluctuation scale of the ground motion is obtained as

$$\alpha_{jj}(z) = \iint_{\xi} \eta_{jj}(\xi_r, \xi_t, z)\, d\xi_r d\xi_t. \tag{7}$$

The fluctuation scale is the most condensed spatial variation parameter. Since it depends especially on the area usually limited in practice, the normalization by the area is adopted for the fluctuation scale to get the appropriate estimate. Then the normalized fluctuation scale with the specified area, A_0, covered by the limited separation vector $\boldsymbol{\xi}$ is

$$\alpha_{0\,jj}(z) = \alpha_{jj}(z)/A_0. \tag{8}$$

Based on the acceleration records, the depth-dependence of these spatial variation parameters is examined in following chapters. The spatial variation parameters, however, can also be defined for velocity and/or displacement records in the same way.

DEPTH-DEPENDENT SPATIAL VARIATION OF GROUND MOTION

In the array observation at the Chiba site (Katayama *et al.*, 1990), fifteen accelerometers installed at GL – 1 m are covering an area of approximately 300 m square, as shown in Fig. 1. The topographical and geological conditions in the site are generally simple and the ground surface is almost flat. In such a condition, this study focuses on the depth-dependence of the spatial variation. Then the analysis is carried out by using the twelve earthquake events in the Chiba array records at GL –1 m, –10 m, and –20 m, as listed in Table 1. At each event, the time windows of 10 seconds for R and T, and 7.5 seconds for U, are analyzed (Δt = 0.005 s), corresponding *P*-wave and *S*-wave parts, respectively.

Data Processing for the Coherence Function and Preliminary Analysis

Point Power Spectrum. A spatial variation of ground motion can be investigated by the power spectrum of each point at the same ground level as likely the coherence function, equivalent in the frequency domain to the space-time earthquake

Table 1. Location of Borehole Accelerometers (○: used, △: unused).

Depth	Borehole														
(m)	C0	C1	C2	C3	C4	P1	P2	P3	P4	P5	P6	P7	P8	P9	P0
1	○	○	○	○	○	○	○	○	○	○	○	○	○	○	○
5	△	△	△	△	△										
10	○	○	○	○	○	○	○	○	○	○	○				
20	○					○	○	○	○	○	○	○	○	○	○
40	△									△					

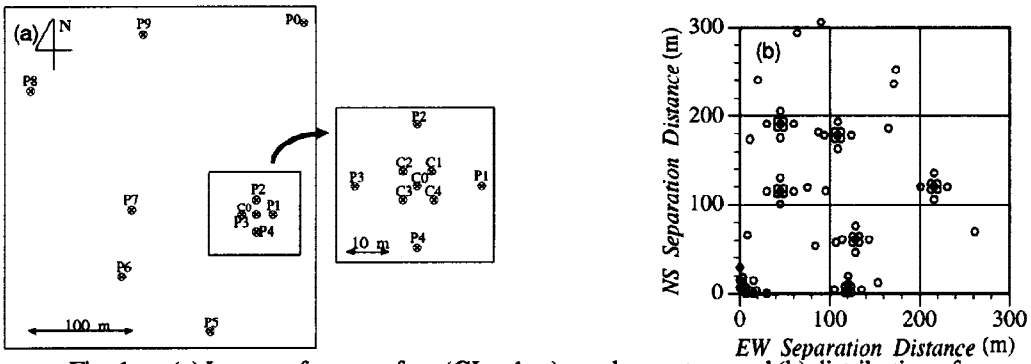

Fig. 1. (a) Layout of near surface (GL – 1 m) accelerometers, and (b) distribution of separation vectors resulting from those 15 combinations.

ground motion. The result for the earthquake event 8519 is used as a typical example. Figure 2 shows the acceleration power spectrum averaged using the records of seven points (C0, P1-P6 in Fig. 1) at the same ground levels, –1 m, –10 m, and –20 m. The top and bottom of this figure show the mean and the C.O.V. of the power spectrum, respectively. Note that for the case using more number of records where the larger area is considered, the similar result is obtained for the mean, whereas the C.O.V. increases as the area increases. It can be seen from the mean of the power spectrum that the amplification of the ground motion differs at each frequency; especially at the frequencies of around 2.5, 4, 6, and 8 Hz. It also can be seen that the amplification for horizontal components is different from that for up-down component because the different time windows are used for the horizontal and up-down components as mentioned above. These results are consistent for the analysis based on the one-dimensional wave propagation theory (Katayama *et al.*, 1990; Lu *et al.*, 1990). The C.O.V. of the power spectrum in the bottom of Fig. 2 is due to the spatial variation of the ground motion. Therefore, the C.O.V. of the power spectrum is considered representing the spatial variation at the specified frequency. Although it is difficult to distinguish the difference of the C.O.V. at each depth level, it can be seen that the C.O.V. increases as the frequency increases. It is expected that the spatial variation of ground motion is increasing in the

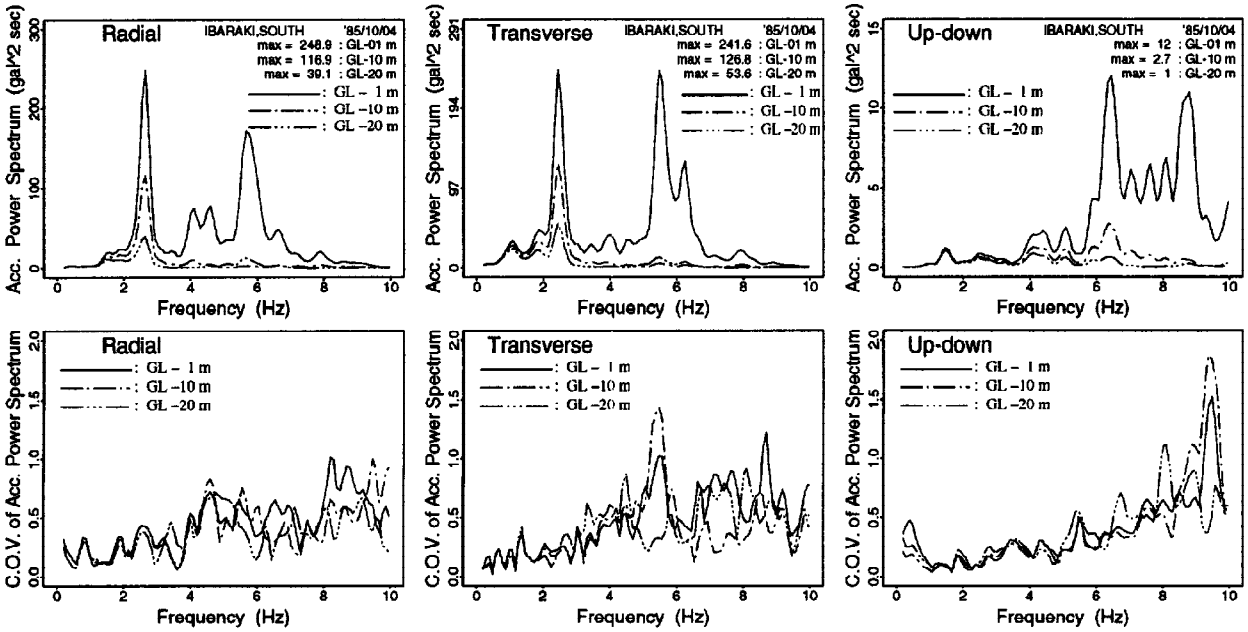

Fig. 2. Acceleration power spectrum at depths of GL –1 m, –10 m, and –20 m for event 8519 (top: mean; bottom: coefficient of variation).

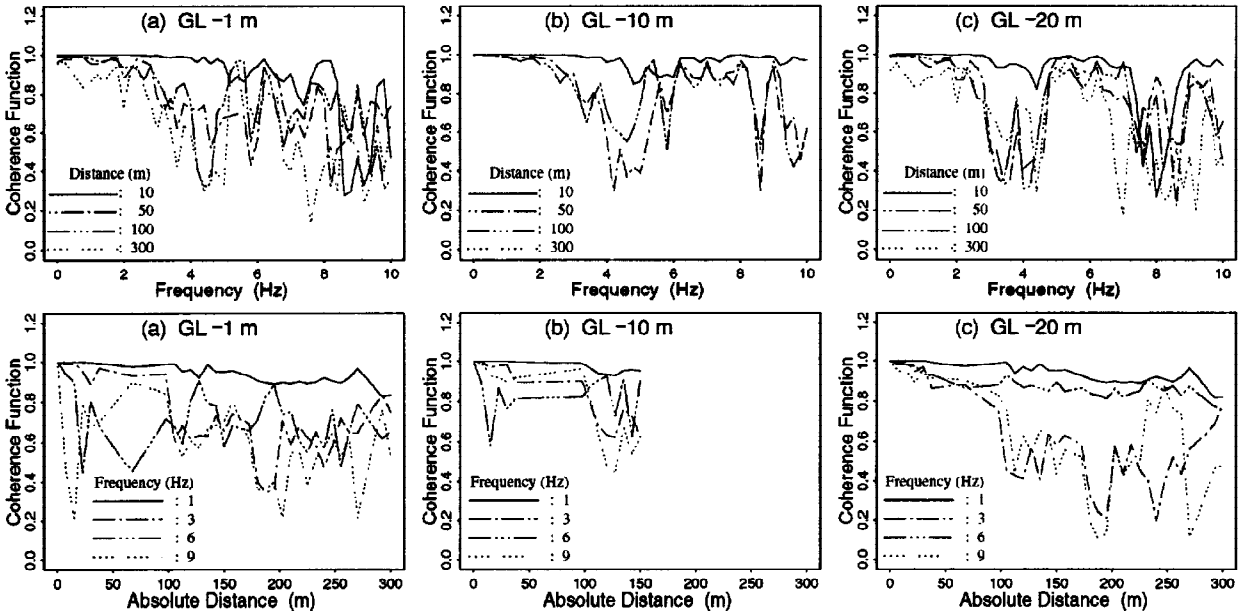

Fig. 3. Coherence function (transverse component of event 8519) interpolated with respect to absolute distance (top: frequency; bottom: distance).

amplification process of the ground motion in the near-surface soil layers. The clear depth-dependence of spatial variation, however, could not be seen from this C.O.V. of the power spectrum at depth levels, 1 m, 10 m, and 20 m.

Data Processing for the Coherence Function. Coherence functions are calculated from pairs of acceleration records assuming their strong motion parts to be statistically homogeneous and stationary. As expected, the coherence function decreases as the frequency and separation distance increase. It is shown that, especially at the dominant frequencies, the coherence function shows a rapid decay only due to the rapid changes of the phase spectrum (Lu *et al.*, 1990). Therefore, local decays are removed and the coherence function model is assumed to be an envelope of coherence function computed in the analysis following Kataoka *et al.* (1990).

Since the coherence function computed in the frequency domain depends strongly on the smoothing of power spectra, specifying the information of the smoothing procedure is important. To remove appropriately the local decays of the coherence function, the power spectrum is smoothed by applying the Parzen's spectral window with a specified bandwidth of 0.4 Hz. To estimate the envelope of the computed coherence function, this study adopts the technique that uses the narrow smoothing bandwidth of the 0.4 Hz and then the local peaks of the coherence function. Then, a nonlinear regression analysis to these peaks is conducted for estimating parameters of the model for the R, T, and U to investigate the difference of the value of model parameters among them. That technique would yield an appropriate engineering estimate for the coherence function (Nakamura and Yamazaki, 1995).

For each event, the coherence function is linearly interpolated as a continuous surface, based on the layout of the near surface (GL –1 m) accelerometers and the distribution of separation vectors resulting from all combinations. The *point* coherence function is computed for all pairs of acceleration records. By the use of the spatial interpolation of the station spacing to be a limited set, the coherence function then can be plotted as a function of both of the frequency and separation distance. As an example, the coherence function is shown in Fig. 3 for the *S*-wave part of the transverse component (event 8519). The coherence function decreases with both frequency and separation distance. Similar results were obtained from the analysis of other events. Note that the distribution of the separation vectors available to estimate the coherence function may not be the same in different spatial ranges as can be seen from Fig. 1. Thus, the confidence in each estimate could vary. In general, less of confidence is associated with the coherence function for larger separation distances.

Coherence Function Model. A Gaussian coherence function model with spatially ellipsoidal correlation structure has been proposed by Nakamura and Yamazaki (1995) for the spatial variation of space-time earthquake ground motion as follows:

$$\gamma_{jj}(\xi_r, \xi_t, f) = e^{-c_0 f} \exp\left\{-\frac{f^2 + {c_3}^2}{{c_1}^2}\left({c_4}^2 {\xi_r}^2 + {\xi_t}^2\right)\right\} + \left(1 - e^{-c_0 f}\right)\exp\left\{-\frac{f^2}{{c_2}^2}\left({c_4}^2 {\xi_r}^2 + {\xi_t}^2\right)\right\} \quad (9)$$

in which c_i's are parameters of the model. The parameter $c_0 f$ indicates decay with frequency at short distances and c_4 a degree of

Table 2. Averaged values of the model parameters regressed by those from each event for the coherence function at each depth.

component	(a) Model parameter for GL −1 m					(b) Model parameter for GL −10 m					(c) Model parameter for GL −20 m				
	c_0 (s)	c_1 (km/s)	c_2 (km/s)	c_3 (Hz)	c_4 (–)	c_0 (s)	c_1 (km/s)	c_2 (km/s)	c_3 (Hz)	c_4 (–)	c_0 (s)	c_1 (km/s)	c_2 (km/s)	c_3 (Hz)	c_4 (–)
Radial	0.0302	74.5	0.0824	58.4	1.01	0.0114	36.2	0.140	50.9	1.03	0.0216	48.0	0.174	48.7	0.90
σ	0.0067	67.5	0.0136	41.9	0.16	0.0042	16.7	0.061	17.3	0.25	0.0036	38.0	0.034	27.1	0.31
Transverse	0.0310	41.2	0.0952	33.6	1.14	0.0152	63.8	0.203	64.6	1.20	0.0213	51.6	0.192	42.6	1.14
σ	0.0049	32.1	0.0226	23.4	0.22	0.0050	51.6	0.058	34.5	0.39	0.0064	58.3	0.037	38.8	0.14
Up-down	0.0069	8.9	0.1069	4.8	0.95	0.0101	7.00	0.116	0.410	1.13	0.0095	7.05	0.113	0.330	0.94
σ	0.0059	8.5	0.0297	11.7	0.19	0.0032	2.88	0.023	0.630	0.21	0.0028	1.59	0.042	0.602	0.30

σ: standard deviation of 12 (for *S*-wave) or 11 (for *P*-wave) samples.

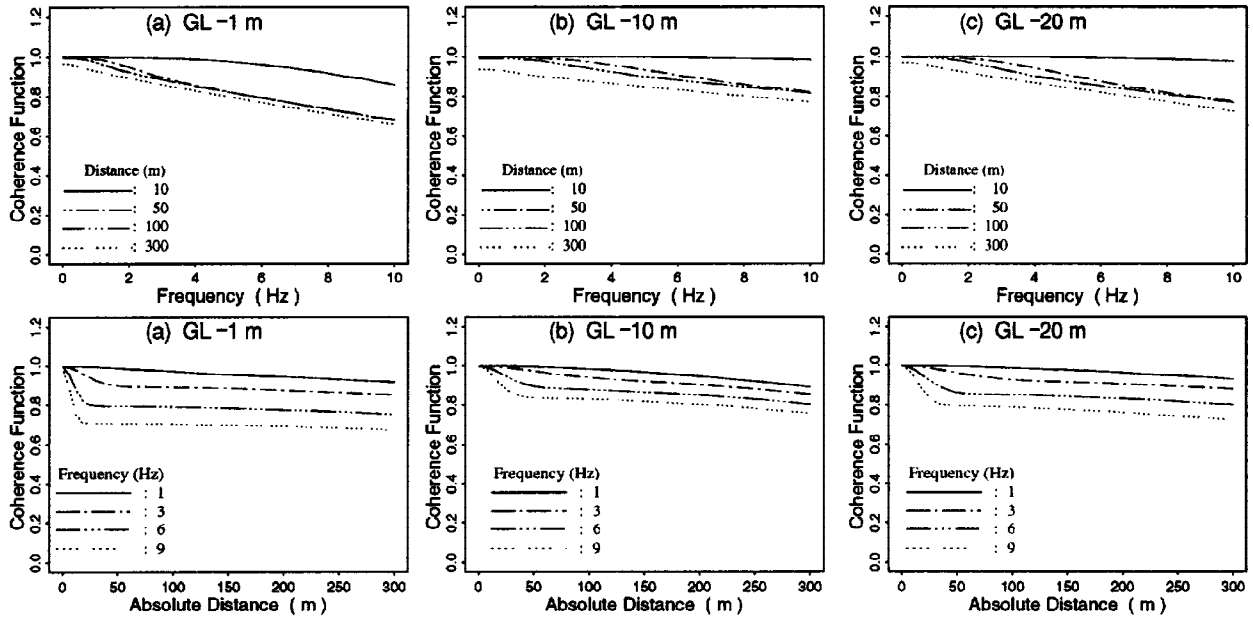

Fig. 4. The coherence function model for transverse component of event 8519 (top: frequency; bottom: distance).

spatial anisotropy. The correlation area of each exponential is assumed as $c_1^2/\left(f^2+c_3^2\right)$ for large distances and as c_2^2/f^2 for short distances. A nonlinear least squares procedure is used to fit this model to the peaks of coherence function computed from the records for each event. The result for each depth level, 1 m, 10 m, and 20 m, is listed in Table 2. Although the model considers the ellipsoidal correlation structure using the parameter c_4, it is found that the results of analysis do not show the significant anisotropic correlation structure of the coherence function model. For the *S*-wave part of the transverse component (event 8519), the model is plotted in Fig. 4, to which the computed coherence function shown in Fig. 3 corresponds.

The correlation area is obtained by integrating the coherence function simply with respect to the separation distance. However, the depth-dependence of the correlation area is not so significant as the C.O.V. of the power spectrum shown in Fig. 2, compared with other spatial variation parameters. The result of the correlation area is not shown in this paper for that reason.

Spatial Variation Parameters at Each Depth: GL −1 m, −10 m, and −20 m

The spatial variation parameters show the average of the information about the spatial variation of the ground motion. In this section, the spatial correlation coefficient and the fluctuation scale are considered as the spatial variation parameters. The spatial correlation coefficient averages the information with respect to the frequency and the fluctuation scale averages the information with respect to the frequency and the separation distance for the spatial variation of the ground motion.

Spatial Correlation Coefficient. Figure 5 shows the mean and C.O.V. of the spatial correlation coefficient calculated for R, T, and U at each depth level, 1 m, 10 m and 20 m. Note that in this case the direction of the separation vector is at 45 degrees from the epicentral direction. The top of Fig. 5 shows that the spatial correlation coefficient decreases steeply at closer separation distances up to about 50 m. The spatial correlation coefficient for U is larger than those for R and T and

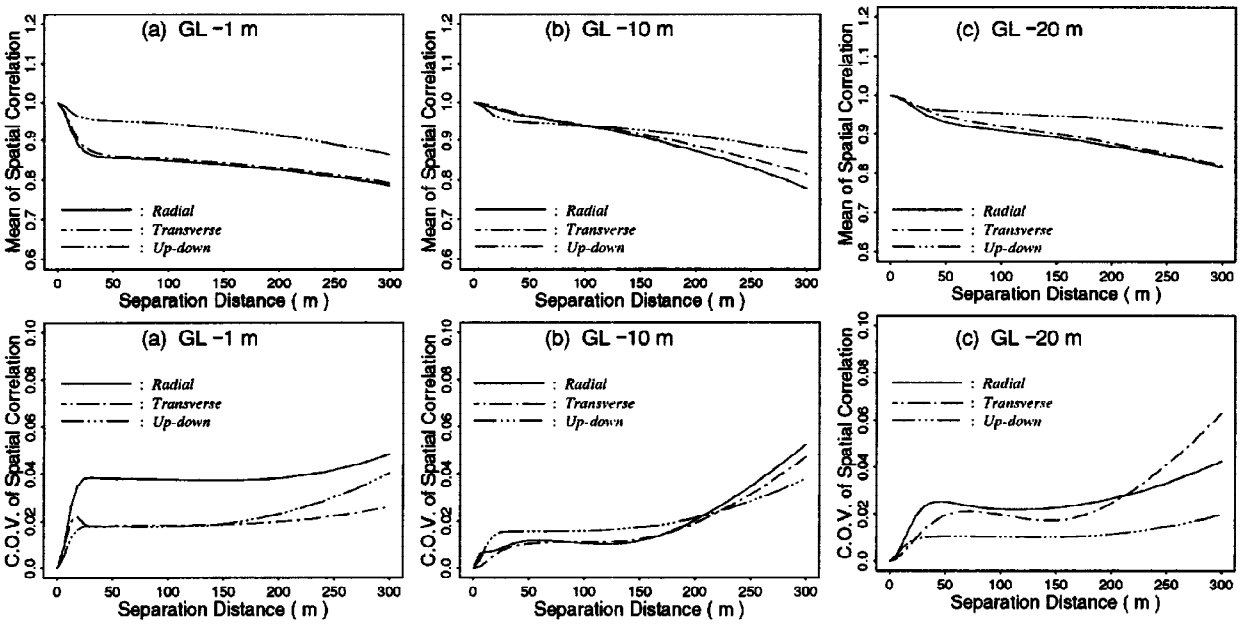

Fig. 5. Spatial correlation coefficient for each depth; GL –1 m, –10 m, and –20 m (top: mean; bottom: coefficient of variation).

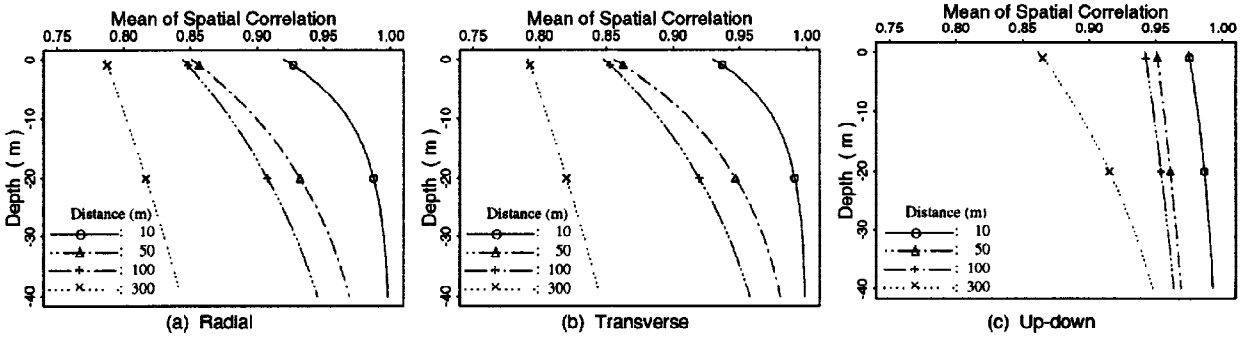

Fig. 6. Mean of spatial correlation coefficient (Hz) at depths of GL –1 m and –20 m and its depth-dependent model for each horizontal distance.

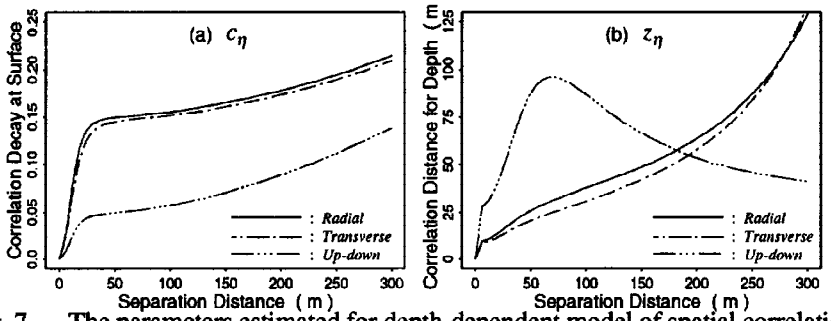

Fig. 7. The parameters estimated for depth-dependent model of spatial correlation coefficient (Hz) at depths of GL –1 m and –20 m.

is close to 1.0 as the depth level increases. This result reflects a tendency of the coherence function. Note that at GL –10 m, the spatial correlation coefficient for R and T do not show a steep decrease at shorter distances, similarly to the coherence function. The C.O.V. of the spatial correlation coefficient in the bottom of Fig. 5 increases with the increase of the separation distance. These results of the spatial correlation coefficient are calculated from the coherence function estimated using the Chiba array records. Accordingly, the results from horizontal arrays at GL – 1 m and –20 m can be used within separation distances up to 300 m, and those from the array at GL –10 m can be used within approximately 150 m. It is complicated to model the spatial correlation coefficient because the number of available data is small. However, the model is proposed as an attempt to investigate trends with respect to depth. The model is restricted by the asymptotic condition, that, the spatial correlation coefficient approaches unity with the increase of the depth, and is shown as

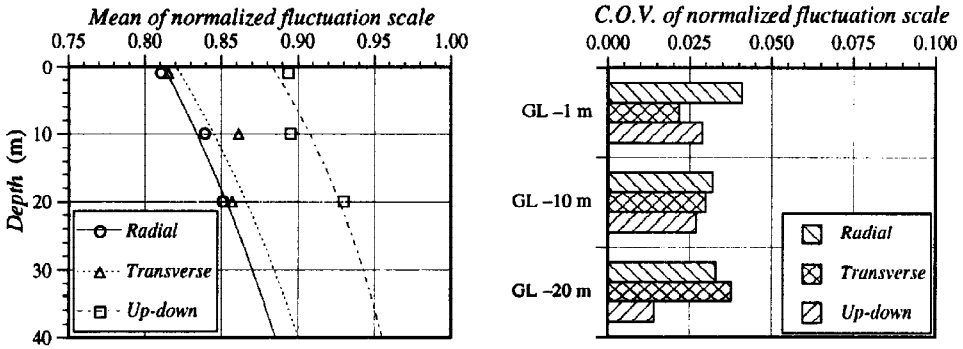

Fig. 8. Mean and C.O.V. of normalized fluctuation scale at depths of GL –1 m, –10 m, and –20 m, and its depth-dependent model.

Table 3. The parameters estimated for depth-dependent model of normalized fluctuation scale.

Vibration component	*Parameters of the model* c_α(–)	z_α(m)	*Coefficient of determination*
Radial	0.188	81.0	0.94
Transverse	0.180	67.9	0.69
Up-down	0.117	41.9	0.85

$$\eta_{jj}(z;\xi_r,\xi_t)=1-c_\eta(\xi_r,\xi_t)\exp\left\{-z/z_\eta(\xi_r,\xi_t)\right\} \tag{10}$$

where $1-c_\eta$ is the value of the spatial correlation coefficient at the ground surface and z_η indicates the correlation depth corresponding to the correlation distance for the depth direction of exponential part of this model.

To make the result for this model clearer, in Fig. 5, the values of the spatial correlation coefficient at GL –1 m and –20 m are used. Fig. 6 shows the mean values of the spatial correlation coefficient in Fig. 5 with its model curves. It is shown that the spatial correlation coefficient for R and T is depth-dependent especially at shorter horizontal distances, whereas that for U is depth-dependent at larger distances. Fig. 7 shows the values of the model parameters. It can be seen from this figure that c_η for all three components increases with the increase of the separation distance. The correlation depth, z_η, increases for R and T as the separation distance increases. z_η for U does not show a monotonic increase but a peak at around 70 m, which corresponds to the end of the decrease at shorter distances.

Normalized fluctuation Scale. The normalized fluctuation scale is equivalent to the fluctuation scale for the random wave divided by that for the coherent wave. The normalized fluctuation scale is computed by numerical integration of a composition of the unit-area point power spectrum and the estimated coherence function in space and frequency domains. Fig. 8 shows the mean and C.O.V. of normalized fluctuation scale for R, T, and U estimated at each depth. Note that for the normalization, the specified area adopted in (8) is considered as 300 m × 300 m in this case. It is found that the normalized fluctuation scale decreases with the increase of the area, because the coherence function decreases with the increase of the separation distance. As the depth increases, each mean of the normalized fluctuation scale approaches unity. The C.O.V.s are generally around 0.025 at all depths. The C.O.V. for T increases and for U it decreases as depth increases. When the number of data is small, a meaningful modeling is very difficult for reasons of sensitivity. However, modeling of the normalized fluctuation scale may be possible due to its asymptotic condition. Considering the results of the analysis and the asymptotic condition for normalized fluctuation scale, the model for the fluctuation scale is proposed as

$$\alpha_{0jj}(z)=1-c_\alpha\exp\left(-z/z_\alpha\right) \tag{11}$$

where $1-c_\alpha$ is the value at the ground surface and z_α indicates the vertical correlation distance normalized fluctuation scale. A weighted least squares analysis is conducted for estimating the parameters of the depth-dependent fluctuation scale model. The weight is considered as the inverse of the C.O.V. of the fluctuation scales that is ranging from 0.014 to 0.040 plotted in Fig. 8 (b).

It can be seen from this model curve in Fig. 8 (a) that the normalized fluctuation scales become larger at deeper levels, although the scale at GL –10 m is slightly different. This result clearly shows that the correlation of the up-down component is higher than that of the horizontal components at each depth. The estimated values of the model parameters are listed in Table 3. At the ground surface, within the extent of the specified area, the observed decrease of the spatial variation for the horizontal and up-down components are around 20 per cent and 10 per cent, respectively. c_α, the normalized fluctuation scale, for R and T is about 0.9 times of that for U. The vertical correlation distance of the model

for R and T is about 1.8 times of that for U. The ground motion even at GL –20 m is spatially varying for R to about 78% {exp (20.0 / 81.0)}, for T to about 74% {exp (20.0 / 67.9)}, and for U to about 62% {exp (20.0 / 41.9)}. Therefore the amount of the spatial variation shallower than depth level 20 m is small but comparable to that deeper than depth level 20 m. It might be affected by the inhomogeneity of a near-surface soil layer.

CONCLUSIONS

Based on a dense array observation, this study shows the basic evidence for further research to understand more realistically the depth-dependent spatial variation of earthquake ground motion over small areas. The spatial variation parameters such as the coherence function, the spatial correlation coefficient, and the fluctuation scale, are analyzed mainly for the space-time earthquake ground motion. Using the coherence function to represent the spatial variation over small areas, it is demonstrated that as the ground level becomes deep, the coherence function increases especially at shorter distances and higher frequencies.

In future, it might be required to compare the spatial variation parameter with the point maximum ground motion parameter, e.g., for the fluctuation scale with the PGA. As the depth increases, the PGA decreases while the fluctuation scale increases. Those trends are significant especially at the near-surface. This result is consistent with our engineering sense that the ground motion is more coherent in the deeper ground level, although at GL –20 m the ground motion is not so coherent. The spatial ground motion parameters proposed here are utilized for the parametric study of the seismic response analysis of spatially extended structures, such as populous large underground facilities.

ACKNOWLEDGMENT

The author would like to express his sincere appreciation to Profs. T. Katayama and F. Yamazaki of the Institute of Industrial Science, the University of Tokyo. This research was financially supported by the Grant-in-Aid for Scientific Research for Japanese Junior Scientists (No. 2827), the Ministry of Education, Science, and Culture.

REFERENCES

Abrahamson, N. A., J. F. Schneider and J. C. Stepp (1991). Empirical Spatial Coherency Functions for Application to Soil-Structure Interaction Analyses. *Earthquake Spectra, 7*, 1-27.

Hao, H. (1989). Effects of Spatial Variation of Ground Motions on Large Multiply-Supported Structures. *Report* No. UCB/EERC-89/06, *Earthquake Engineering Research Center, University of California, Berkeley.*

Harada, T. (1984). Probabilistic Modeling of Spatial Variation of Strong Earthquake Ground Displacements. *Proceedings of 8th World Conference on Earthquake Engineering, II*, 605-612.

Harichandran, R. S. and E. H. Vanmarcke (1986). Stochastic Variation of Earthquake Ground Motion in Space and Time. *Journal of Engineering Mechanics Division, Proc. ASCE, 112*, 154-174.

Kataoka, N., H. Morishita and A. Mita (1990). Spatial Variation of Seismic Ground Motion at Lotung Soil-Structure Interaction Experiment Site. *Proceedings of the 8th Japan Earthquake Engineering Symposium, 1*, 607-612.

Katayama, T., F. Yamazaki, S. Nagata, L. Lu and T. Turker (1990). A Strong Motion Database for the Chiba Seismometer Array and its Engineering Analysis. *Earthquake Eng. Struct. Dyn., 19*, 1089-1106.

Katayama, T. (1991). Use of Dense Array Data in the Determination of Engineering Properties of Strong Motions. *Structural Safety, 10*, 27-51.

Loh, C. H. and Y. T. Yeh (1988). Spatial Variation and Stochastic Modelling of Seismic Differential Ground Movement. *Earthquake Eng. Struct. Dyn., 16*, 583-596.

Lu, L., F. Yamazaki and T. Katayama (1990). Soil Amplification Based on the Chiba Array Database. *Proceedings of the 8th Japan Earthquake Engineering Symposium, 1*, 511-516.

Lu, L, T. Annaka, M. Shimada and M. Fujitani (1994). Analysis and Modeling of Spatial Coherence of Earthquake Ground Motions. *Proceedings of 4th U.S. National Conference on Earthquake Engineering, III*, 199-208.

Menke, W., A. L. Lerner-Lam and R. Mithal (1991). Spatial Coherence of 5-25 Hz Seismic Wavefields at a Hard Rock Site. *Struct. Safety, 10*, 163-179.

Nakamura, H. and F. Yamazaki (1995). Spatial Variation of Earthquake Ground Motion Based on Dense Array Records. *Transaction of the 13th International Conference on Structural Mechanics in Reactor Technology, III*, 19-24.

Sato, T. and H. Kawase (1992). Finite Element Simulation of Seismic Wave Propagation in Near-surface Random Media, *Proceedings of the International Symposium on the Effects of Surface Geology on Seismic Motion, I*, 257-262.

Sawada, T. and H. Kameda (1988). Modeling of Nonstationary Cross Spectrum for Multivariate Earthquake Motions by Multifilter Technique. *Proceedings of 9th World Conference on Earthquake Engineering, II*, 795-800.

Vanmarcke, E. (1983). *Random Fields: Analysis and Synthesis*. MIT Press, Cambridge, MA.